

MANUFACTURE OF FUNCTIONALLY GRADIENT MATERIALS USING WELD-DEPOSITION

S. Suryakumar* and M. A. Somashekara*

* Indian Institute of Technology Hyderabad, Hyderabad, India – 502205

Abstract

When the inherent inhomogeneity of Additive Manufacturing techniques is carefully exploited, the anisotropy transforms into the desired distribution of the properties paving the way for manufacture of Functionally Gradient Materials. The present work focuses on using weld-deposition based Additive Manufacturing techniques to realize the same. Mechanical properties like hardness and tensile strength can be controlled by a smaller degree through control of process parameters like current, layer thickness etc. A wider control of material properties can be obtained with the help of tandem weld-deposition setup like twin-wire. In tandem twin-wire weld-deposition, two filler wires (electrodes) are guided separately and it is possible to control each filler wire separately. The investigations done on these two approaches are presented in paper.

1. Introduction

Additive Manufacturing (AM) originally known as rapid prototyping, is a process of making three dimensional objects directly from a digital model. Owing to the slicing methodology employed in their manufacture, objects created from these techniques are inhomogeneous or non-uniform, i.e., they are inherently anisotropic. When this inherent nature is carefully exploited, the anisotropy transforms into the desired distribution of the properties.

Functionally gradient objects have composition and microstructure change gradually over a volume, resulting in a corresponding change in the properties of the material. Initially interest in fabrication of FGMs was limited to polymer nano composites and various biomedical and bone replacements applications [1]. Subsequently, research into fabrication of metallic FGMs is also being actively explored. Laminated Object Manufacturing [2–4], Selective Laser Sintering (SLS) [5–7], Selective Laser Melting [8,9], Ultrasonic Consolidation [10,11], Laser cladding-based techniques[12–14], and 3D Printing of ZCorp [15] are some of the present processes which are capable of realizing a gradient matrix.

2. Functionally Gradient Materials by Additive Manufacturing: State of art

Additive manufacturing process can directly manufacture the product or component with CAD model as input. Based on material deposition method, additive manufacturing can be classified in Laminated Manufacturing, Powder bed technology and deposition technologies (Figure 1). The following are some of the methods explored by researcher for realizing FGM:

Laminated object manufacturing (LOM) is one of popular rapid prototyping and manufacturing process. Only the boundaries are addressed instead of other process like interiors, therefore process speed depends on surface area object instead of volume. Fabrication of FMGs using Ultrasonic consolidation (UC) is one of laminated manufacturing process, combining ultrasonic metal seam welding and CNC milling. First object is built up on a rigidly held plate bolted on to a heated platen, with temperature ranging from room temperature to a maximum of approximately 200°C. Parts are built layer by layer from bottom to top and excess material removed by using CNC machine. Fabrications of FGMs were done by joining of different metallic foils together by using ultrasonic welding [10].

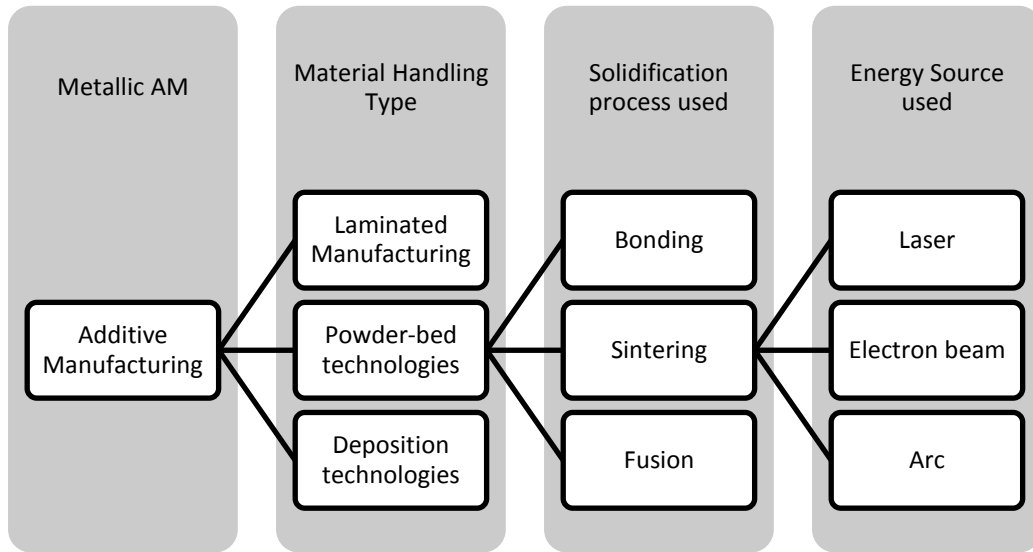


Figure 1: Classification of Additive Manufacturing Methods

Selective laser sintering was originally developed by University of Texas, Austin. It is presently marketed by 3D systems, USA and EOS, Germany. Selective laser sintering (SLS) is one of popular AM process with an ability to manufacture three dimensional functional product of any complicated shape using metal powder, scanning the laser beam at the desired locations to get the three dimensional functional part. Gu et al., demonstrated the ability of SLS to manufacture composite materials with WC-10% particulate reinforced Cu matrix [7].

Laser Engineering Net Shaping (LENS) originally developed by Sandia National Laboratories USA, is capable of producing variety of FGMs including functionally graded TiC/Ti composite material [11]. FGMs from LENS process are used some of application like load bearing implants [12].

SDM laser deposition system developed at Stanford University, is capable of producing functionally graded metals through the use of powder mixing. While Shape Deposition Manufacturing has always had the capability to produce multi material artifacts, powder mixing enables the deposition of single layers in which material properties can be smoothly varied without discrete interfaces between dissimilar materials. Fessler et.al studied functional gradient

material deposition to construct an advanced injection molding tool which transitions from Invar in the center to stainless steel on the outside [16].

3. Manufacturing of FGMs using arc-deposition

Based on the energy source used, AM techniques can be classified as those using Laser, electron beam or arc (Figure 1). Arc based weld-deposition techniques offer unique advantages due to their ability to control the properties of the deposited matrix through the control of process parameters like current, layer thickness etc. Earlier, researchers from IIT Bombay used a CNC machine to control the weld-deposition path in a process referred as Hybrid Layered Manufacturing (HLM) [17–19]]. The current work at IIT Hyderabad, presented here combines a weld-deposition to a Kuka robot for motion control.

Functionally gradient matrix can be obtained in arc-deposition process using the following two approaches:

- by varying process parameter
- by use of multiple wires in a twin wire welding

The focus of the present paper is use of process parameters to get the desired variation of mechanical properties, like hardness in the object. Hardness of material is important in the mechanical properties. Earlier researcher studied the influence of current on hardness. From previous study it is clear that mechanical properties of the object are dependent on the weld-deposition parameters. Hence it is possible to achieve desired mechanical properties at a point through the careful control of the weld-deposition parameters.

3.1 Experimental Setup

Gas Metal Arc Welding (GMAW) of Time Twin weld deposition comprises of two separate wires, in which controllable digital power sources work independently - with two separate filler wires - in just one gas nozzle creating a common weld pool, as shown in Figure 2.

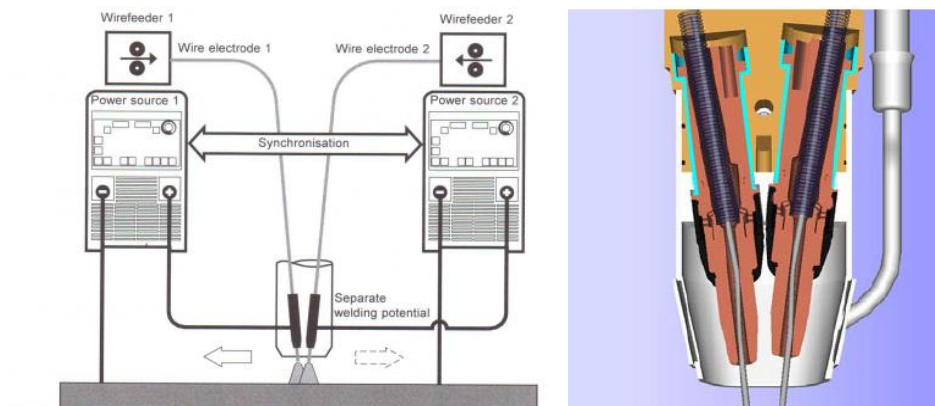


Figure 2: Time Twin weld-deposition system

Experiments were done to understand the relationship between input and output parameter for single bead for various values of welding current and torch speed. The range of twin wire weld deposition has been carried out with stable arc. To find the range of current and torch speed of twin wire weld deposition for additive manufacturing several trails, as shown in Figure 3 have been carried out. Through visual assessment, it was found that a stable weld-deposition could be carried out in the range {80A to 160A} and {0.6m/min to 2.84m/min} for current and torch speed respectively. ER 70S-6 copper coated mild steel wire of 0.8mm diameter, and composition as listed in Table 1, was used as filler wire.

Table 1: Chemical composition of ER 70S-6 filler wire.

Element	C	Mn	Si	P	S	Al
Composition (%)	0.22	0.3	0.3	0.012	0.007	1.3

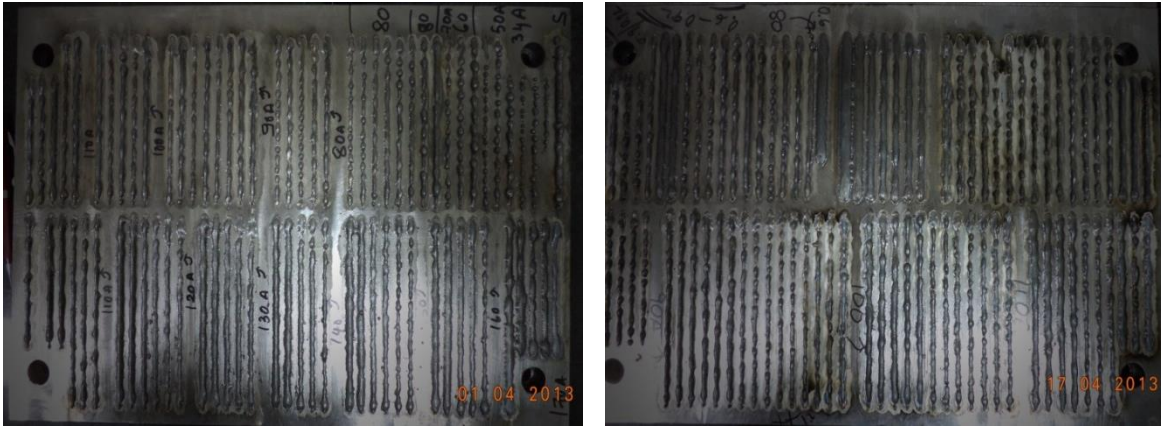


Figure 3: Conducted weld trails for current and torch speed.

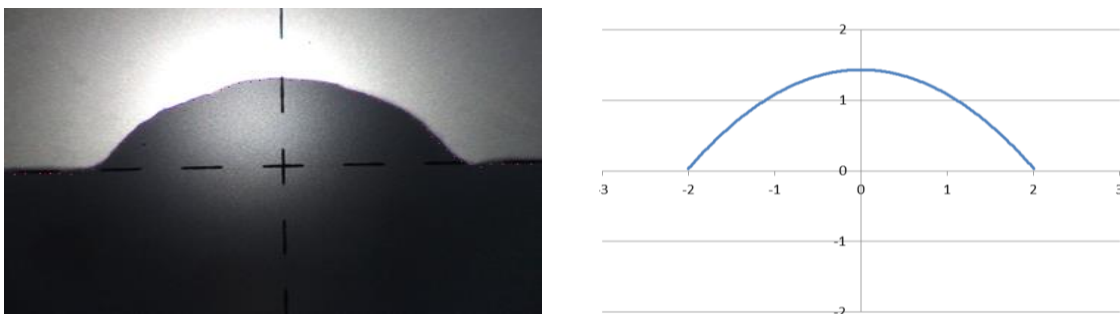


Figure 4: Geometry of weld bead (a) bead cross-section from profile projector
(b) reconstructed parabola from collected points

3.2 Geometry of the weld bead

Prediction of the geometric shape of the weld-bead is an important criterion in selection the right set of process parameters to obtain a desired layer thickness. Bead profile is also

important in identifying the optimal stepover increment. Aiyiti et. al., in their analysis using plasma arc welding have assumed the beads as overlapping circular arcs and arrived at the most desirable scan spacing [20]. Suryakumar et al., approximated the bead-profile to a symmetric parabola and found that the optimal stepover increment is two-third of the weld bead width [18]. The Figure 4 shows the sample cross section of a bead profile; the left taken from the profile projector and the right the curve reconstructed from the measured points. It is clear from the figure that the bead profile for twin-wire is closer to parabola and hence the same has been selected.

A pattern shown in Figure 5 was deposited on a MS substrate of 200 mm x 150mm x 10mm for various combinations of current and torch speed. This pattern is such that the initial beads preheat the substrate so that middle bead is representative of the actual working conditions. In other words, only the middle bead is used for the measurements. Table 2 lists out the process parameters used for the same.

The area of the parabolic bead with width, w and height, h is given by the expression:

$$A_{measured} = \frac{2wh}{3}$$

Similarly, the area of bead cross section predicated based on the volume of material coming out of the welding torch can be written as:

$$A_{predicted} = \frac{2\pi V_w d^2}{4V_t}$$

where, d is the diameter of the filler wire, V_w and V_t are the wire and torch speeds respectively. Table 3 gives the measured and predicted set of values for these various combinations of current and torch speed. Figure 6 shows the area of bead from predicated and area of measured, plotted against the 45° line. This reveals a good fit between measured and predicted cross section profile, enabling the selection of appropriate values of current and torch speed for a desired bead size.

Table 2: Process parameter used in twin wire weld deposition

Current (A)	80 - 160
Wire Speed (m/min)	5.4 - 12.5
Torch Speed(m/min)	0.6 - 2.84
Nozzle gap (base plate to torch)	12mm
Shielding gas flow rate (L/min)	16
Shielding gas	82% Argon+18% CO2

Table 3: Comparison of Predicated and experimental areas of the weld bead.

Sl	Current I (Amp)	Wire speed V_r (m/min)	Torch speed V_t (m/min)	Width w (mm)	Height h (mm)	Area of weld bead (mm ²)		% error
						Measured $A = \frac{2wh}{3}$	Predicated $A = \frac{2\pi V_w d^2}{4V_t}$	
1	80	5.4	0.60	5.94	2.23	8.84	9.04	-2.30
2	80	5.4	0.83	5.08	2.02	6.85	6.58	3.95
3	80	5.4	1.05	4.22	1.84	5.18	5.17	0.22
4	100	7.1	0.92	6.09	2.05	8.31	7.80	6.14
5	100	7.1	1.31	4.70	1.87	5.86	5.47	6.66
6	120	9.0	0.89	6.74	2.25	10.09	10.16	-0.74
7	120	9.0	1.39	5.53	1.77	6.52	6.53	-0.12
8	120	9.0	1.90	4.61	1.60	4.91	4.76	3.01
9	140	10.8	1.38	6.01	1.93	7.72	7.89	2.23
10	140	10.8	2.03	5.41	1.64	5.92	5.36	9.46
11	160	12.5	1.26	7.30	2.04	9.93	9.97	-0.36
12	160	12.5	2.05	5.57	1.48	5.48	6.13	-11.81
13	160	12.5	2.84	5.52	1.26	4.65	4.42	4.83



Figure 5: Weld patterns with different current and torch speeds

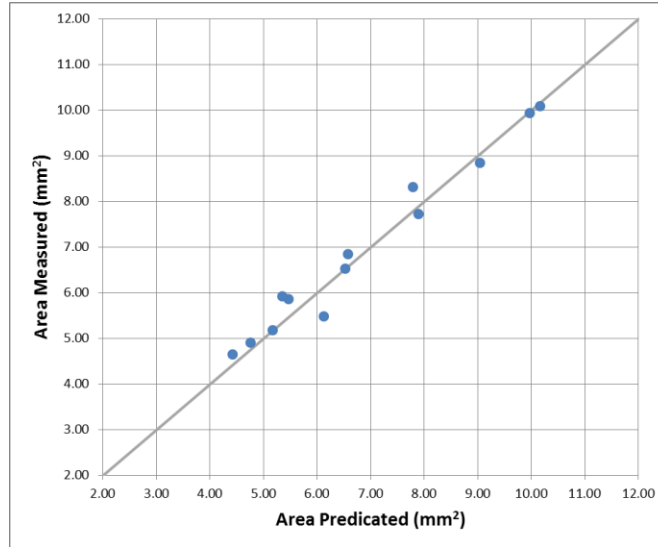


Figure 6: Predicted vs. measured cross-sectional areas of the weld bead.

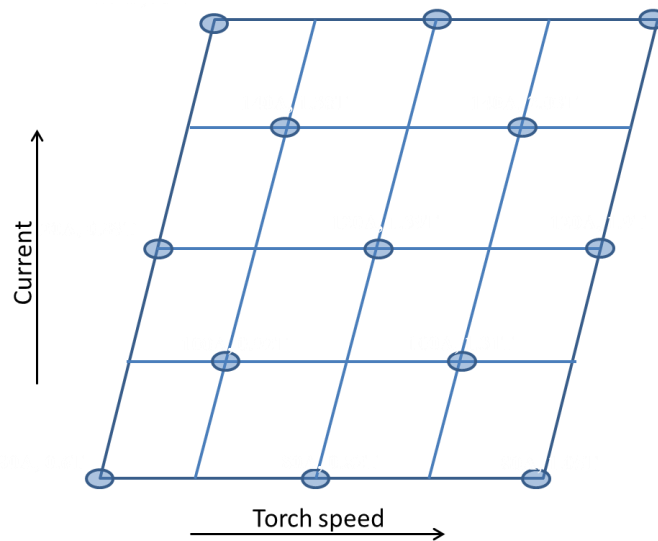


Figure 7: Various values of current and torch speed selected to generate the expression for prediction of hardness

3.3 Hardness

A series of experiments were carried out to understand the effect of process parameters on the Hardness of the weld-deposition. In order to be able to generate an equation for predicting the hardness value in terms of current and torch speed, a set of 13 points covering the surface of the operating range, as shown in Figure 7 were selected. These are the same of set of patterns and combinations used for the earlier analysis of bead crosssection. The micro-hardness values, in values Vickers Pyramid Number (HVN) units was measured using a Emco make micro hardness tester. Before the hardness testing, the weld bead surface needs to be polished. The samples has

been ground with emery paper of finer grits of 180, 360, 600, 1200, 1500, 2000 and finally diamond polished using the 9 μ , 6 μ , 3 μ and 1 μ grits. The samples were placed in the Ethanol chemical solution and heated up to 10min for removing unwanted particle on the bead surface. Finally a diamond indenter of load 0.5kgf and 15 sec indent time was used to make a dent on the polished surface. Figure 8 depicts the polished surface and the indent after the diamond indentation.



Figure 8: (a) A polished weld bead samples (b) diamond indent display of diagonal and hardness values

Table 4: Hardness values from experimentation

Sl	Current (Amp)	Wire speed (m/min)	Torch speed (m/min)	Hardness (HV)
1	80	5.4	0.60	240.83
2	80	5.4	0.83	250.20
3	80	5.4	1.05	261.30
4	100	7.1	0.92	229.63
5	100	7.1	1.31	274.00
6	120	9.0	0.89	237.44
7	120	9.0	1.39	264.80
8	120	9.0	1.90	319.89
9	140	10.8	1.38	261.00
10	140	10.8	2.03	270.71
11	160	12.5	1.26	228.83
12	160	12.5	2.05	255.13
13	160	12.5	2.84	260.50

4. Results and Validation

The measured values of the hardness for the various combinations of current and torch speed is given in Table 4. Based on these values, a second degree regression model for predicting Hardness, H as a function of current, I (in Amps) and torch speed V_t (in m/min) was generated using *LABFit*:

$$H = B_0 + B_1 * I + B_2 * V_t + B_3 * I^2 + B_4 * V_t^2 + B_5 * I * V_t$$

$$B_0 = 0.13721224947E + 03$$

$$B_1 = 0.28864573360E + 00$$

$$B_2 = 0.17674581268E + 03$$

$$B_3 = 0.13691821344E - 03$$

$$B_4 = -0.50856556814E + 01$$

$$B_5 = -0.84264097114E + 00$$

The surface plot the Hardness against current and torch speed based on the above equation is generated using MatLab is shown in Figure 9. To validate the equation generated from regression analysis, two set of points at random locations were chosen. The measured hardness for these points was compared to the value predicted from the above equation. These values are shown in Table 5. The error was found to be 6.5% and 4.2%, indicating a good resemblance and thus validating the regression model.

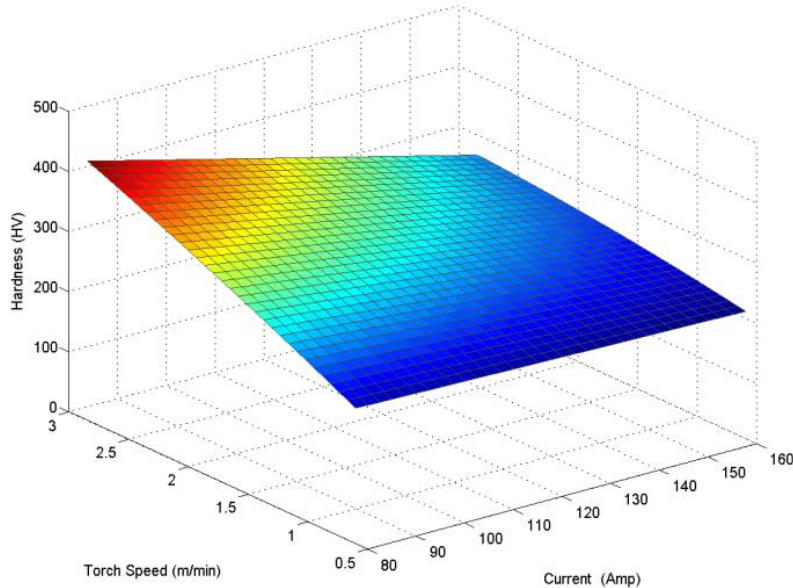


Figure 9: Hardness, H as a function of current and torch speed

Table 5: Hardness values for validation points

Sl	Current (Amp)	Torch speed (m/min)	Geometrical parameters			Hardness (HV)		Error (%)
			Height (mm)	Width (mm)	Area (mm ²)	Measured experimentally	Predicted from the regression fit	
1	110	1.24	5.21	1.90	6.58	250.5	267.02	-6.5
2	130	1.55	5.80	1.78	6.90	258.11	268.9	-4.2

5. Conclusion

The feasibility of realizing a functionally gradient matrix using a twin-wire based weld-deposition system has been explored. In this approach, it is possible to get the desired distribution of properties by (i) varying the process parameters and/or (ii) controlling the proportion of different fillers wire.

After identifying the operating range of process parameter viz., current and torch speed, the bead profile was analyzed assuming its crosssection to be a symmetric parabola. A second order regression equation for predicting the Hardness as a function of current and torch speed was generated based on a series of experiments. The micro-hardness of these specimen, in Vickers Pyramid Number (HVN) units and measured using a diamond indenter of load 0.5kgf was used for the same. The regression equation has been validated by comparing the measured and predicted values of hardness for a set of two new points.

The future work in this area will explore the implementation of archiving a wider range of mechanical properties through use of multiple wires of different composition and varying the proportion of each to get the desired distribution of properties.

References

- [1] Pompe W., Worch H., Epple M., Friess W., Gelinsky M., Greil P., Hempel U., Scharnweber D., and Schulte K., 2003, "Functionally graded materials for biomedical applications," *Mater. Sci. Eng.*, 362(1–2), pp. 40–60.
- [2] Zhang Y., Han J., Zhang X., He X., Li Z., and Du S., 2001, "Rapid prototyping and combustion synthesis of TiC/Ni functionally gradient materials," *Mater. Sci. Eng.*, 299(1–2), pp. 218–224.
- [3] Tari M. J., Bals A., Park J., Lin M. Y., and Thomas Hahn H., 1998, "Rapid prototyping of composite parts using resin transfer molding and laminated object manufacturing," *Compos. Part Appl. Sci. Manuf.*, 29(5–6), pp. 651–661.
- [4] Klosterman D., Chartoff R., Graves G., Osborne N., and Priore B., 1998, "Interfacial characteristics of composites fabricated by laminated object manufacturing," *Compos. Part Appl. Sci. Manuf.*, 29(9–10), pp. 1165–1174.
- [5] Chung H., and Das S., 2008, "Functionally graded Nylon-11/silica nanocomposites produced by selective laser sintering," *Mater. Sci. Eng.*, 487(1–2), pp. 251–257.
- [6] Chung H., and Das S., 2006, "Processing and properties of glass bead particulate-filled functionally graded Nylon-11 composites produced by selective laser sintering," *Mater. Sci. Eng.*, 437(2), pp. 226–234.
- [7] GU D., SHEN Y., DAI P., and YANG M., 2006, "Microstructure and property of sub-micro WC-10 %Co particulate reinforced Cu matrix composites prepared by selective laser sintering," *Trans. Nonferrous Met. Soc. China*, 16(2), pp. 357–362.
- [8] Beal V. E., Erasenthiran P., Ahrens C. H., and Dickens P., 2007, "Evaluating the use of functionally graded materials inserts produced by selective laser melting on the injection moulding of plastics parts," *Proc. Inst. Mech. Eng. Part B J. Eng. Manuf.*, 221(6), pp. 945–954.

- [9] Mumtaz K. A., and Hopkinson N., 2007, "Laser melting functionally graded composition of Waspaloy® and Zirconia powders," *J. Mater. Sci.*, 42(18), pp. 7647–7656.
- [10] Kumar S., 2010, "Development of Functionally Graded Materials by Ultrasonic Consolidation," *Cirp J. Manuf. Sci. Technol.*, 3(1), pp. 85–87.
- [11] Domack M. ., and Baughman J. ., 2005, "Development of nickel-titanium graded composition components," *Rapid Prototyp. J.*, 11(1), pp. 41–51.
- [12] Bandyopadhyay A., Krishna B., Xue W., and Bose S., 2009, "Application of Laser Engineered Net Shaping (LENS) to manufacture porous and functionally graded structures for load bearing implants," *J. Mater. Sci. Mater. Med.*, 20(0), pp. 29–34.
- [13] Pei Y. ., and De Hosson J. T. ., 2000, "Functionally graded materials produced by laser cladding," *Acta Mater.*, 48(10), pp. 2617–2624.
- [14] Pei Y. ., and De Hosson J. T. ., 2001, "Five-fold branched Si particles in laser clad AlSi functionally graded materials," *Acta Mater.*, 49(4), pp. 561–571.
- [15] Jackson T. R., Liu H., Patrikalakis N. M., Sachs E. M., and Cima M. J., 1999, "Modeling and designing functionally graded material components for fabrication with local composition control," *Mater. Des.*, 20(2–3), pp. 63–75.
- [16] Merz R., F B P., K R., M T., and L,E W., 1994, "Shape Deposition Manufacturing," *Proceedings of the Solid Freeform Fabrication Symposium.*, The University of Texas at Austin.
- [17] Karunakaran K. P., Bernard A., Suryakumar S., Dembinski L., and Taillandier G., 2012, "Rapid manufacturing of metallic objects," *Rapid Prototyp. J.*, 18(4), pp. 264–280.
- [18] Suryakumar S., Karunakaran K. P., Bernard A., Chandrasekhar U., Raghavender N., and Sharma D., 2011, "Weld bead modeling and process optimization in Hybrid Layered Manufacturing," *Comput.-Aided Des.*, 43(4), pp. 331–344.
- [19] Karunakaran K., Suryakumar S., Pushpa V., and Akula S., 2009, "Retrofitment of a CNC machine for hybrid layered manufacturing," *Int. J. Adv. Manuf. Technol.*, 45(7), pp. 690–703.
- [20] Aiyiti W., Zhao W., Lu B., and Tang Y., 2006, "Investigation of the overlapping parameters of MPAW-based rapid prototyping," *Rapid Prototyp. J.*, 12(3), pp. 165–172.